



Clinical Feasibility of Synthetic Magnetic Resonance Imaging in the Diagnosis of Internal Derangements of the Knee

Jisook Yi, MD*, Young Han Lee, MD, Ho-Taek Song, MD, Jin-Suck Suh, MD

All authors: Department of Radiology, Research Institute of Radiological Science, YUHS-KRIBB Medical Convergence Research Institute, and Severance Biomedical Science Institute, Yonsei University College of Medicine, Seoul 03722, Korea

Objective: To evaluate the feasibility of synthetic magnetic resonance imaging (MRI) compared to conventional MRI for the diagnosis of internal derangements of the knee at 3T.

Materials and Methods: Following Institutional Review Board approval, image sets of conventional and synthetic MRI in 39 patients were included. Two musculoskeletal radiologists compared the image sets and qualitatively analyzed the images. Subjective image quality was assessed using a four-grade scale. Interobserver agreement and intersequence agreement between conventional and synthetic images for cartilage lesions, tears of the cruciate ligament, and tears of the meniscus were independently assessed using Kappa statistics. In patients who underwent arthroscopy ($n = 8$), the sensitivity, specificity, and accuracy for evaluated internal structures were calculated using arthroscopic findings as the gold standard.

Results: There was no statistically significant difference in image quality ($p = 0.90$). Interobserver agreement ($\kappa = 0.649$ – 0.981) and intersequence agreement ($\kappa = 0.794$ – 0.938) were nearly perfect for all evaluated structures. The sensitivity, specificity, and accuracy for detecting cartilage lesions (sensitivity, 63.6% vs. 54.6–63.6%; specificity, 91.9% vs. 91.9%; accuracy, 83.3–85.4% vs. 83.3–85.4%) and tears of the cruciate ligament (sensitivity, specificity, accuracy, 100% vs. 100%) and meniscus (sensitivity, 50.0–62.5% vs. 62.5%; specificity, 100% vs. 87.5–100%; accuracy, 83.3–85.4% vs. 83.3–85.4%) were similar between the two MRI methods.

Conclusion: Conventional and synthetic MRI showed substantial to almost perfect degree of agreement for the assessment of internal derangement of knee joints. Synthetic MRI may be feasible in the diagnosis of internal derangements of the knee.

Keywords: Synthetic MRI; Knee; Cruciate ligament; Meniscus; Cartilage

Received December 21, 2016; accepted after revision August 12, 2017.

This work was supported by a National Research Foundation (NRF) grant funded by the Korea government, Ministry of Science, ICT & Future Planning (MSIP, 2015R1A2A1A05001887).

Corresponding author: Young Han Lee, MD, Department of Radiology, Research Institute of Radiological Science, YUHS-KRIBB Medical Convergence Research Institute, and Severance Biomedical Science Institute, Yonsei University College of Medicine, 50-1 Yonsei-ro, Seodaemun-gu, Seoul 03722, Korea.

• Tel: (822) 2228-7420 • Fax: (822) 393-3035

• E-mail: radiologie@gmail.com

*Current address: Department of Radiology, Inje University College of Medicine, Haeundae Paik Hospital, Busan 48108, Korea.

This is an Open Access article distributed under the terms of the Creative Commons Attribution Non-Commercial License (<http://creativecommons.org/licenses/by-nc/4.0>) which permits unrestricted non-commercial use, distribution, and reproduction in any medium, provided the original work is properly cited.

INTRODUCTION

Magnetic resonance imaging (MRI) is important in the diagnosis of internal derangements of knee (IDK) due to its excellent tissue contrast (1). MRI is also used to evaluate treatment response, including pharmacologic and surgical therapy (2). The knee joint is a complex arrangement of cruciate ligaments, menisci, cartilage, and musculotendinous structure. Sagittal plane images play a key role in evaluating cruciate ligaments and meniscal anatomy (3). A more detailed evaluation of the complex course of cruciate ligament and complex meniscal tear requires multiplanar imaging. The imaging time (scan time) is usually long for knee MRI (4–6). The radiologist should select imaging pulse sequences and planes within a limited

time; a routine knee protocol for IDK includes T2-weighted fast spin echo (FSE) sequence or proton density (PD)-weighted FSE sequence in two or three orthogonal planes, and at least one T1-weighted sequence is usually used for ligamentous structures, including articular cartilage, and meniscus and bone lesions (1, 7, 8).

Synthetic MRI is a novel method that generates T1-weighted, T2-weighted, PD-weighted, and inversion recovery images based on MR quantification (relaxation times and PD) within a single scan (9). The settings of echo time (TE), repetition time (TR), and inversion time (TI) can be modified by the reader (9). Several investigations that have used synthetic MR sequences in brain images have revealed acceptable image quality and artifacts, and suggested the clinical utility of the method (9-14).

We hypothesized that synthetic MRI can be used for investigations of the knee that requires several pulse sequences. No published study has assessed musculoskeletal imaging using synthetic MRI in a clinical setting. We conducted this study to evaluate the feasibility of synthetic MRI compared to conventional MRI for the diagnosis of IDK.

MATERIALS AND METHODS

This study was approved by the Institutional Review Board and informed consent was waived due to the retrospective nature of the study. Between March 2016 and September 2016, 50 consecutive patients underwent both synthetic and conventional knee MRI at our institution. Among them, 11 patients were excluded: six patients underwent knee MRI using a pediatric protocol, four patients were in

a postoperative state (three cases of partial meniscectomy and one case involving reconstruction of the anterior cruciate ligament [ACL]), and one patient had fracture and hemarthrosis of the knee joint (Fig. 1). In total, 39 patients were eligible. They included 25 women (aged 20–80 years; mean age, 48.6 years) and 14 men (aged 22–77 years; mean age, 53.4 years). Among the 39 patients, eight (seven women and one man) underwent arthroscopic surgery, meniscectomy (n = 7), cartilage shaving (n = 4), and reconstruction of the ACL (n = 1) (Fig. 1).

MRI

Magnetic resonance imaging was performed using a 3T MR system (Discovery 750w; GE Healthcare, Waukesha, WI, USA) with a 16-channel GEM flex-medium flexible coil (NeoCoil, Pewaukee, WI, USA). Conventional two-dimensional (2D) sagittal, T2-weighted FSE images, with periodically rotated overlapping parallel lines using the enhanced reconstruction (PROPELLER) technique, were obtained using the following imaging parameters: TR, 8760–8800 ms; TE, 138–142 ms; field of view (FOV), 140 x 140 mm; image matrix, 512 x 512; slice thickness, 3 mm (interslice gap, 0.3 mm); flip angle, 160°; and echo train length, 24. The image acquisition time was 4 minutes 5 seconds. Conventional fat-suppressed three-dimensional (3D) isotropic FSE PD-weighted images were acquired using the following imaging parameters: TR, 1200 ms; TE, 30 ms; FOV, 144 x 144 mm; image matrix, 320 x 320; slice thickness, 1 mm; and echo train length, 46. The image acquisition time was 7 minutes 35 seconds. A multiple-dynamic multiple echo sequence was performed using the following imaging parameters in

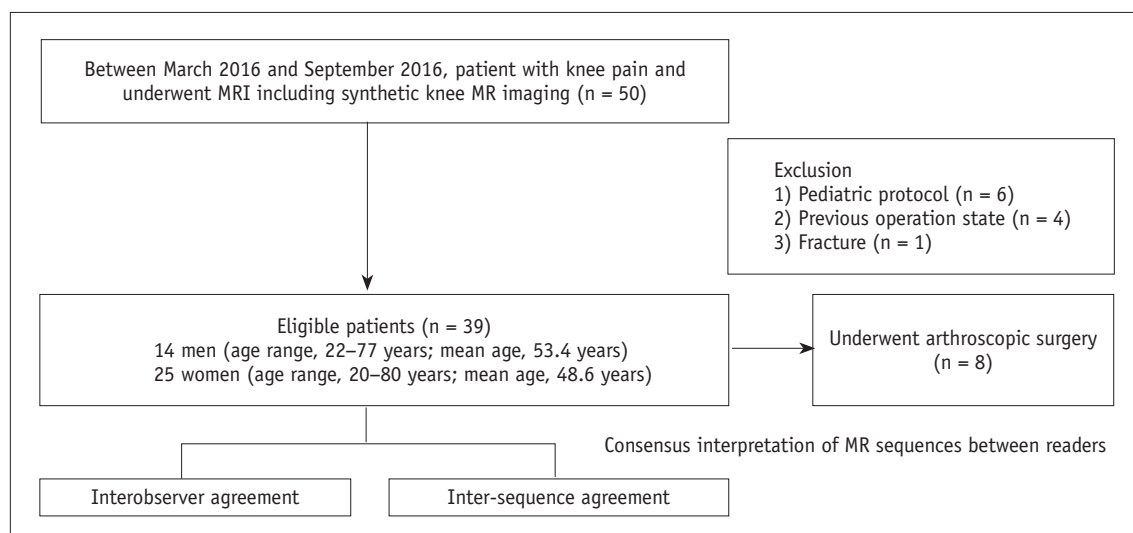


Fig. 1. Study flow diagram. MRI = magnetic resonance imaging

a sagittal orientation for synthetic reconstruction (MAGiC; GE Healthcare): TR, 4384 ms; TE, 21.952 and 98.784 ms; four TI, 175, 700, 1930, and 4210 ms; FOV, 160 x 160 mm; acquisition matrix, 320 x 256; slice thickness, 3 mm (interslice gap, 1 mm); flip angle, 90° and 110°; and echo train length, 14. The image acquisition time was 6 minutes 20 seconds. The synthetic T2-weighted images were generated with the same TR and TE of conventional 2D T2-weighted sequence (TR 8760–8800 ms, TE 138–142 ms) for comparison. Synthetic PD-weighted images were generated using a standardized setting (TR 8000 ms, TE 10 ms) within the software.

Imaging Interpretation

All synthetic MRI (both T2-weighted and PD-weighted FSE sequences in sagittal orientation) and conventional MRI (both 2D T2-weighted FSE and 3D fat-suppressed isotropic PD-weighted FSE sequences in sagittal orientation) scans were retrospectively reviewed by two musculoskeletal radiologists (with 10 and 2 years of experience in musculoskeletal radiology, respectively) in a random order to reduce bias. The reviewers were blind to electronic medical records, including the results of physical examinations, arthroscopic findings, and diagnosis. All images were digitally assessed by using a commercially available PACS workstation Centricity® Radiology RA1000 (GE Healthcare, Barrington, IL, USA).

Image Quality

The subjective image quality of the four MR images (conventional 2D T2-weighted FSE sequence, conventional 3D fat-suppressed PD-weighted FSE sequence, and synthetic T2-weighted FSE sequence, synthetic PD-weighted FSE sequence) was rated on a four-grade scale by one reader: 1) cartilage delineation, 2) ligament delineation, 3) meniscus delineation, and 4) artifact. Quality criteria were excellent (minimal artifacts or image-quality issues, cartilage/ligament/meniscus were sharply delineated), good (minimal artifacts or image-quality issues, one or two of the previously mentioned structures were less than optimally delineated), acceptable (acceptable image quality for diagnostic purposes but noticeable artifacts or image-quality issues), and poor (extensive artifacts or noise, substantial limitation in the delineation of the above mentioned structures) (15).

Definitions

A cruciate ligament tear was defined as complete or partial discontinuity or indistinct margins of the ligament, with or without signal change (16–18). A meniscal tear was defined as the presence of abnormal signal intensity within the meniscus that extended to the meniscal articular surface, or an abnormal morphologic contour of the meniscus (19). The presence of a meniscal tear was recorded on a meniscus-to-meniscus basis. The reader recorded the presence or absence of a meniscal tear even if multiple meniscal tears were noted.

The articular cartilage was evaluated according to its location within six compartments: medial femoral condyle, lateral femoral condyle, medial tibial plateau, lateral tibial plateau, trochlea, and patella. The cartilage lesion grades were defined according to the modified Noyes classification system (20). Grade 0 was normal. Grade 1 displayed signal intensity abnormality, but intact surface. Grade 2 displayed superficial partial-thickness cartilage lesion comprising less than 50% of the total thickness of the articular surface. Grade 3 displayed deep partial-thickness cartilage lesion greater than 50% but less than 100% of the total thickness of the articular surface. Grade 4 displayed, full-thickness cartilage lesion extending to the subchondral bone. The highest grade lesion in a compartment was rated by the readers.

Arthroscopic Knee Surgery

Arthroscopic findings were considered the reference standard. The eight patients underwent arthroscopic knee surgery within 6 months after MRI (range, 5–173 days; mean \pm standard deviation, 50.9 \pm 51.9 days). All arthroscopic knee surgeries were performed by two orthopedic surgeons specialized in knee arthroscopy, with 25 and 7 years of clinical experience, respectively. From the operative and arthroscopic notes, we recorded the cartilage lesion grades and the presence or absence of ACL, posterior cruciate ligament (PCL), medial meniscus (MM), and lateral meniscus (LM) tears.

Statistical Analyses

Subjective image quality was compared among the four MR sequences in both of conventional and synthetic images with the Kruskal-Wallis and Mann-Whitney U tests. After independent assessment of the cruciate ligament, meniscus, and articular cartilage, the two readers formed a consensus interpretation on each of conventional (combined

2D T2-weighted and 3D fat-suppressed PD-weighted FSE sequences) and synthetic MR (T2-weighted and PD-weighted FSE sequences) images to compare the agreement between conventional and synthetic images.

Cohen's Kappa statistics were performed to evaluate the interobserver agreement and intersequence agreement. A $\kappa < 0$ indicated no agreement, $0 < \kappa \leq 0.2$ indicated slight agreement, $0.2 < \kappa \leq 0.4$ indicated fair agreement, $0.4 < \kappa \leq 0.6$ indicated moderate agreement, $0.6 < \kappa \leq 0.8$ indicated substantial agreement, and $0.8 < \kappa \leq 1$ indicated almost perfect agreement (21). Spearman correlation was used to evaluate the intersequence correlation for cartilage lesions. The sensitivity, specificity, and accuracy for evaluating tears of cruciate ligaments and menisci, and cartilage lesions were calculated on the conventional and synthetic T2-weighted images, using arthroscopy as the gold standard. The McNemar test was used to evaluate the concordance between two imaging sequences and arthroscopic diagnosis for each reader. To compare the cartilage lesion to arthroscopy, cartilage lesions were dichotomized: grade 0 and 1 represented no lesion; and grade 2–4 represented a true lesion.

All statistical analyses were performed using SPSS software version 23 (IBM Corp., Armonk, NY, USA) and R programming environment (R package version 2.3.1, R Foundation of Statistical Imaging, Vienna, Austria; <http://cran.r-project.org>). A p value < 0.05 was considered statistically significant.

RESULTS

All synthetic MRI scans were successfully reconstructed with no significant artifacts. In the evaluation of subjective image quality, conventional T2-weighted FSE MRI showed highest mean ranks (81.04), followed by 3D fat-suppressed PD-weighted FSE images (78.85), synthetic T2-weighted FSE MRI scans (77.19), and synthetic PD-weighted FSE images (76.92). No significant differences were evident among all four imaging approaches ($p = 0.90$). Overall image quality was good to excellent (Fig. 2).

Interobserver agreement and intersequence agreement ranged from substantial to almost perfect for all evaluated structures (Table 1, Figs. 3, 4). Comparison data between conventional and synthetic MRI images in grading cartilage lesion are summarized in Table 2. Compared with the conventional MRI findings, 3 of 20 (15%) grade 1 lesions, 4 of 27 (14.8%) grade 2 lesions, 2 of 23 (8.7%) grade 3 lesions, and 2 of 25 (8.0%) grade 4 lesions were underestimated on synthetic MRI. Three of 139 (2.2%) grade 0 lesions, 2 of 20 (10.0%) grade 1 lesions, 1 of 27 (3.7%) grade 2 lesion, and 3 of 23 (13.0%) grade 3 lesions were overestimated on synthetic MRI (Table 2). There was strong correlation between conventional and synthetic MRI in the evaluation of cartilage lesions ($r = 0.945$, $p = 0.001$). Several additional structures had high concordance between the readers in both conventional and synthetic MRI; these included mucoid degeneration of the ACL ($n = 8$), mucoid degeneration of the PCL ($n = 3$), intra-tendinous ganglion cyst of the ACL ($n = 1$), and the presence of discoid

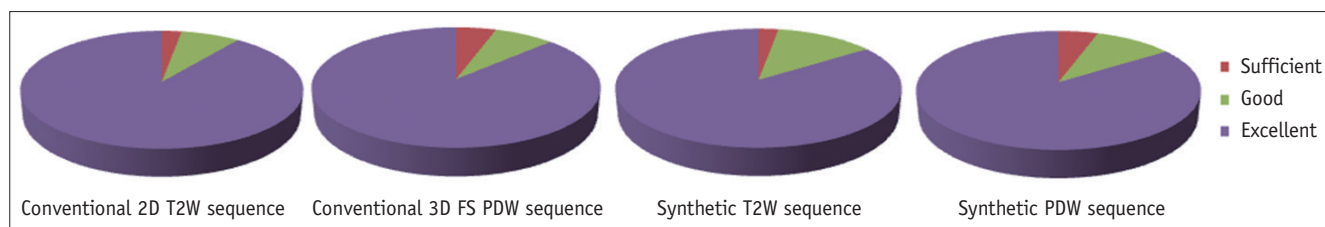


Fig. 2. Comparison of image quality. FS = fat-suppressed, PDW = proton density-weighted, T2W = T2-weighted, 2D = two-dimensional, 3D = three-dimensional

Table 1. Interobserver and Intersequence Agreements for Evaluated Structures

| Parameter | Interobserver Agreement | | Inter-Sequence Agreement* |
|-----------|------------------------------|---------------------------|---------------------------|
| | Conventional MR (κ) | Synthetic MR (κ) | |
| Ligament | 0.649 | 0.741 | 0.794 |
| Meniscus | 0.810 | 0.909 | 0.938 |
| Cartilage | 0.882 | 0.981 | 0.893 |

*Inter-sequence: between conventional MR (2D T2W FSE sequence and 3D fat-suppressed PD-weighted FSE sequence) and synthetic MR (T2W sequence and PD-weighted sequence) images. FSE = fast spin echo, MR = magnetic resonance, PD = proton density, T2W = T2-weighted, 2D = two-dimensional, 3D = three-dimensional

Synthetic MR Image of Knee

meniscus (n = 3).

Arthroscopy revealed one ACL tear, two MM tears, six LM tears, and ten cartilage lesions among 48 cartilage compartments (Table 3). Table 4 lists the sensitivity,

specificity and accuracy of the conventional and synthetic MR images in diagnosing the cartilage lesion (sensitivity, 63.6% vs. 54.6–63.6%, $p = 1$; specificity, 91.9% vs. 91.9%, $p =$ not applicable; accuracy, 83.3–85.4% vs. 83.3–85.4%, p

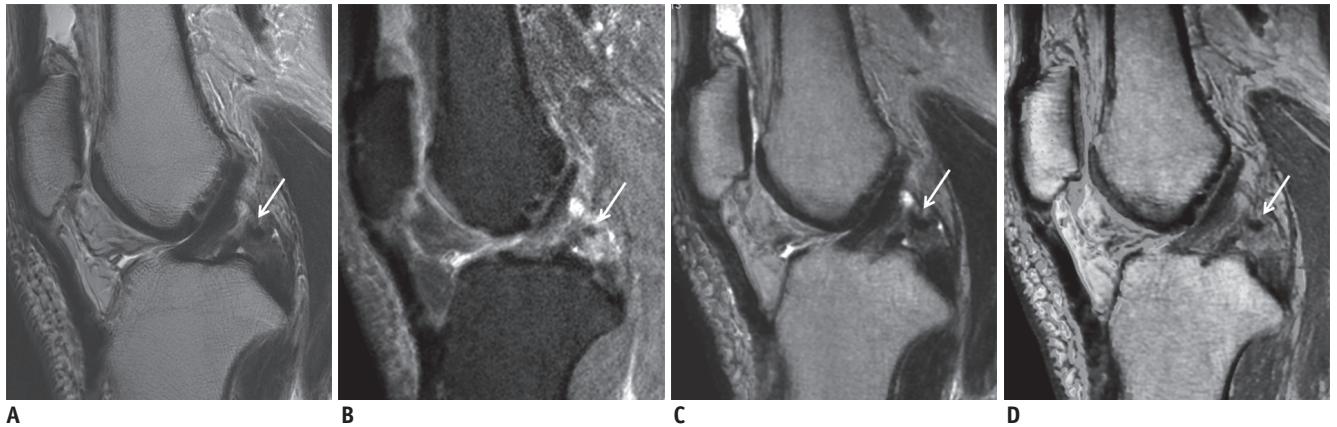


Fig. 3. Normal ACL and complete tear of PCL: findings concordant between conventional and synthetic MR sequence images. 74-year-old male with knee pain. ACL shows normal appearing contour without evidence of signal alternation on conventional 2D T2W (A), 3D fat suppressed PD-weighted (B) sequences, T2W (C) and PD-weighted (D) synthetic MR images. PCL shows increased signal intensity and discontinuity at mid portion (arrow) on conventional MR (A, B) and synthetic MR (C, D) images. ACL = anterior cruciate ligament, MR = magnetic resonance, PCL = posterior cruciate ligament, PD = proton density

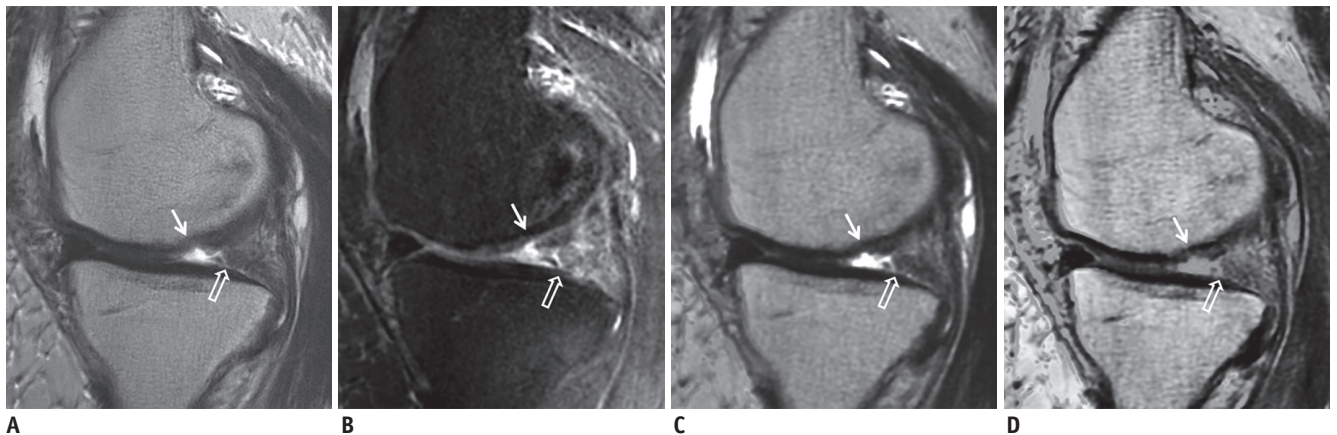


Fig. 4. MM and MFC: findings concordant between conventional and synthetic MR images. 75-year-old female patient with knee pain for 5 months. Abnormal signal intensity within posterior horn of MM with abnormal morphologic contour (open arrow) was noted on conventional 2D T2W (A) and 3D fat-suppressed PD-weighted (B) sequences, T2W (C) and PD-weighted (D) synthetic MR images by both readers. Also, cartilage lesion (defect more than 50% in total depth; arrow) at MFC was noted on all of conventional (A, B) and synthetic (C, D) MR sequences by both readers. Arthroscopy revealed tear of MM and cartilage lesion at MFC. MFC = medial femoral condyle, MM = medial meniscus

Table 2. Comparison between Conventional and Synthetic MR Image for Grading Cartilage Lesions

| Cartilage Lesion | Grade | Conventional MR | | | | | Total (n) |
|------------------|-------|-----------------|----|----|----|----|-----------|
| | | 0 | 1 | 2 | 3 | 4 | |
| Synthetic MR | 0 | 136 | 3 | 3 | 0 | 0 | 142 |
| | 1 | 1 | 15 | 1 | 1 | 0 | 18 |
| | 2 | 2 | 2 | 22 | 1 | 1 | 28 |
| | 3 | 0 | 0 | 0 | 18 | 1 | 19 |
| | 4 | 0 | 0 | 1 | 3 | 23 | 27 |
| Total (n) | | 139 | 20 | 27 | 23 | 25 | 234 |

= 1), tears of the cruciate ligament (sensitivity, specificity, and accuracy, 100% vs. 100%, $p =$ not applicable for sensitivity and specificity, $p = 1$ for accuracy) and meniscus

(sensitivity, 50.0–62.5% vs. 62.5%, $p =$ not applicable; specificity, 100% vs. 87.5–100%, $p = 1$; accuracy, 83.3–85.4% vs. 83.3–85.4%, $p = 1$). Both readers showed

Table 3. Comparison of MRI and Operative Findings for Both Readers

| Parameter | Conventional MR (%) | | Synthetic MR (%) | | Operation (%) |
|------------------|---------------------|-----------|------------------|-----------|---------------|
| | Reader 1 | Reader 2 | Reader 1 | Reader 2 | |
| Ligament | | | | | |
| Normal | 15 (93.8) | 15 (93.8) | 15 (93.8) | 15 (93.8) | 15 (93.8) |
| Tear | 1 (6.2) | 1 (6.2) | 1 (6.2) | 1 (6.2) | 1 (6.2) |
| Meniscus | | | | | |
| Normal | 11 (68.8) | 12 (75.0) | 10 (62.5) | 11 (68.8) | 8 (50.0) |
| Tear | 5 (31.2) | 4 (25.0) | 6 (37.5) | 5 (31.2) | 8 (50.0) |
| Cartilage | | | | | |
| Normal | 39 (81.3) | 38 (79.1) | 38 (79.1) | 39 (81.3) | 38 (79.1) |
| Defect | 9 (18.7) | 10 (20.9) | 10 (20.9) | 9 (18.7) | 10 (20.9) |

Table 4. Sensitivity, Specificity, and Accuracy of Conventional and Synthetic MR Imaging in Detection of Cruciate Ligament Tear, Meniscal Tear, and Cartilage Lesion

| Parameter | Conventional MR | | Synthetic MR | |
|------------------|---------------------|---------------------|---------------------|---------------------|
| | Reader 1 | Reader 2 | Reader 1 | Reader 2 |
| Ligament | | | | |
| Sensitivity | 1 (0.796–1.000) | 1 (0.796–1.000) | 1 (0.796–1.000) | 1 (0.796–1.000) |
| Specificity | 1 (0.207–1.000) | 1 (0.207–1.000) | 1 (0.207–1.000) | 1 (0.207–1.000) |
| Accuracy | 1 (0.806–1.000) | 1 (0.806–1.000) | 1 (0.806–1.000) | 1 (0.806–1.000) |
| Meniscus | | | | |
| Sensitivity | 0.625 (0.306–0.863) | 0.500 (0.215–0.785) | 0.625 (0.306–0.863) | 0.625 (0.306–0.863) |
| Specificity | 1 (0.676–1.000) | 1 (0.676–1.000) | 0.875 (0.529–0.978) | 1 (0.676–1.000) |
| Accuracy | 0.813 (0.570–0.934) | 0.750 (0.505–0.898) | 0.750 (0.505–0.898) | 0.813 (0.570–0.934) |
| Cartilage | | | | |
| Sensitivity | 0.636 (0.354–0.848) | 0.636 (0.354–0.848) | 0.636 (0.354–0.848) | 0.546 (0.280–0.787) |
| Specificity | 0.919 (0.787–0.972) | 0.919 (0.787–0.972) | 0.919 (0.787–0.972) | 0.919 (0.787–0.972) |
| Accuracy | 0.833 (0.704–0.913) | 0.854 (0.728–0.928) | 0.854 (0.728–0.928) | 0.833 (0.704–0.913) |

Data are presented as parameters with 95% confidence intervals in parentheses.

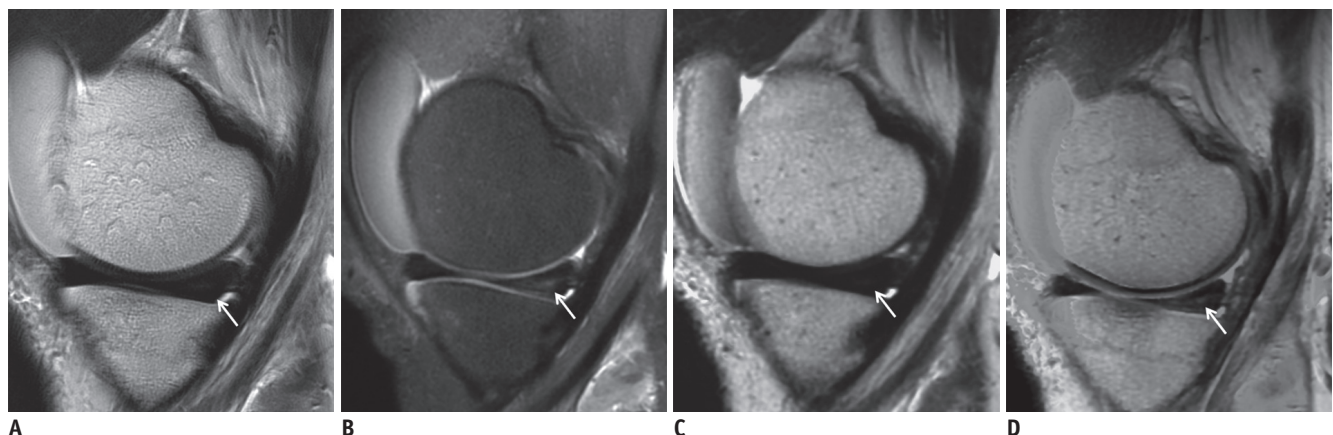


Fig. 5. MM: false negative but concordant between conventional and synthetic MR images.

23-year-old female patient with knee trauma underwent MRI. Subtle increased signal intensity within posterior horn of MM (arrow) without definite evidence of extension to articular side was noted on conventional 2D T2W (A) and 3D fat-suppressed PD-weighted (B) sequences, T2W (C) and PD-weighted (D) synthetic MR images by both readers, and considered not tear. Arthroscopy revealed vertical tear of MM.

similar sensitivity, specificity, and accuracy for all evaluated structures on both MR sequences. There was one false-negative case of a MM tear that was considered by both readers on both sequences as an increase in signal intensity without evidence of a tear that extended to the articular side. It was confirmed as a vertical tear on arthroscopy (Fig. 5). One false-positive diagnosis of an MM tear included a case with synthetic images from reader 1. There were two false-negative cases of an LM tear (which were confirmed as vertical tears on arthroscopy) on both conventional and synthetic images by both readers. Reader 1 assigned three false-positive and five false negative diagnoses of cartilage lesions on the conventional MR image, and three false-positive and four false-negative diagnoses of cartilage lesions on the synthetic MR image. Reader 2 assigned three false-positive and four false-negative diagnoses of cartilage lesions on the conventional MR image, and three false-positive and five false-negative diagnoses of cartilage lesions on the synthetic MR image.

DISCUSSION

Fast imaging is an inevitable issue in MRI, even with recent advancements in MRI scanners (22-25). Although the scan time in conventional image sequences has been reduced, quantitative imaging techniques including cartilage mapping and T2/T1rho mapping are now being included in routine knee protocols (26-28), which require longer scan times. Thus, acceleration of the overall MRI procedure is important to reduce the entire scan time. Moreover, for knee joint imaging, multiplanar imaging and multi-spectral MRI (T1-weighted, T2-weighted, and PD-weighted images) are necessary to evaluate complex internal structures and requires a relatively long scan time. Long scan times increase the costs and limit the number of patients for whom MRI is necessary. From the viewpoint of patient comfort, reducing the scan time is helpful. Patients can experience boredom or discomfort during scans, and the scanned images sometimes suffer from motion artifacts.

Synthetic MRI is a promising and feasible acceleration MRI technique. With synthetic MRI, radiologists can review multi-contrast images in a single scan. The contrast of the images can also be changed with a post-processing step. A synthetic MR sequence image is not affected by scanner setting, radiofrequency field B_1 inhomogeneity, and coil sensitivity, which makes it possible to compare the absolute signal intensity values, signal differences, and contrast in

the same patient, as well as T1 and T2 relaxation times (10). This enables the generation of T1-weighted, T2-weighted, PD-weighted, and inversion recovery images in a single scan, resulting in different tissue contrast with one acquisition, and can also possibly reduce the entire MR scan time.

In the current study, we applied synthetic MRI to knee joint imaging. The results of a side-by-side comparison of conventional and synthetic images in the sagittal plane of the knee joint showed no statistically significant differences in overall image quality and no significant artifacts. In the evaluation of the ACL and PCL in particular, synthetic MRI had similar diagnostic performance to previous studies using conventional T2-weighted or intermediate-weighted sequences (29-31). However, the diagnostic performances of synthetic and conventional MRI were lower than previous analyses of meniscal tears and cartilage lesions (29-31). There are several possible explanations for these findings. First, the number of confirmed arthroscopy cases were too small ($n = 8$), resulting in wide numerical variation, even with the small number of false negative or false positive cases. Second, we only compared sagittal images of meniscus and cartilage lesions, whereas previous studies assessed sagittal, coronal, and axial images (29-31). This may explain the relatively lower sensitivity, specificity, and accuracy for detecting meniscal tears and cartilage lesions, which need to be evaluated in multiplanar imaging including axial, sagittal, and coronal planes (32). Moreover, all false negative cases of meniscal tears (one medial meniscal tear and two lateral meniscal tears) were confirmed as vertical tears by arthroscopy. It is often difficult to detect the peripherally-located vertical tear in MRI due to the surrounding complex anatomy and posterior attachments (33). This situation could be improved by analyzing coronal or axial planes instead of sagittal planes.

Our results suggest that synthetic MRI may be feasible for clinical application in the evaluation of IDK. However, standardized settings within software for soft tissue contrasts (i.e., T2-weighting) were not exactly equal to those on conventional images. For this initial feasibility study, we used the same TR and TE for comparison of the conventional T2-weighted MRI and generated PD image using a standardized setting within the software, although one strength of the synthetic MRI is a tunable TR and TE. In our study, the same TR and TE did not produce the same image contrast. This indicates that synthetic MR images need to be optimized for tissue-stressed T2-

weighted images, which could provide optimal diagnostic performance. The optimized TR and TE are not yet known, and optimized TR and TE depend on the tissue of ligaments and meniscus. Therefore, further studies are needed for optimization of specific TR and TE for different target tissues.

This study has several limitations. First, we compared only sagittal images of conventional and synthetic MRI to evaluate IDK, and therefore it was not exactly same as current clinical setting, which evaluates internal structures of knee joint on multiplanar images. However, the overall interobserver and intersequence agreements between conventional and synthetic images in sagittal plane did not differ. Further studies evaluating including coronal and/or oblique coronal plane are needed. Second, relatively small number of pathologies of cruciate ligament and meniscal tears, and cartilage lesions were included, and few were confirmed with surgical findings. This might limit the generalization of the results. However, the aim of this study was not to validate the diagnostic performance of synthetic MRI, but to evaluate the feasibility of synthetic MRI compared to conventional MRI to diagnosis the internal derangements of the knee. Third, we obtained conventional sequences with the PROPELLER technique, a radial k-space sampling concept that enables correcting motion artifact and the imaging scan time is slightly longer without this technique (34). Conventional MRI with Cartesian k-space might equal those with radial k-space sampling. But the scan time is clinically acceptable, and there was no significant difference in overall image quality between synthetic MRI and conventional MRI.

In conclusions, conventional and synthetic MRI showed a substantial to almost perfect degree of agreement for the assessment of internal derangement of knee joint and may be feasible in the diagnosis of internal derangement of the knee.

REFERENCES

1. Fritz RC. MR imaging of meniscal and cruciate ligament injuries. *Magn Reson Imaging Clin N Am* 2003;11:283-293
2. Crema MD, Roemer FW, Marra MD, Burstein D, Gold GE, Eckstein F, et al. Articular cartilage in the knee: current MR imaging techniques and applications in clinical practice and research. *Radiographics* 2011;31:37-61
3. Stoller DW. *Magnetic resonance imaging in orthopaedics and sports medicine, Volume 1*, 3rd ed. Ambler, PA: Lippincott Williams & Wilkins, 2007:307
4. Duc SR, Zanetti M, Kramer J, Käch KP, Zollkofer CL, Wentz KU. Magnetic resonance imaging of anterior cruciate ligament tears: evaluation of standard orthogonal and tailored paracoronal images. *Acta Radiol* 2005;46:729-733
5. Roberts CC, Towers JD, Spangehl MJ, Carrino JA, Morrison WB. Advanced MR imaging of the cruciate ligaments. *Radiol Clin North Am* 2007;45:1003-1016, vi-vii
6. Kim HS, Yoon YC, Park KJ, Wang JH, Choe BK. Interposition of the posterior cruciate ligament into the medial compartment of the knee joint on coronal magnetic resonance imaging. *Korean J Radiol* 2016; 17:239-244
7. Fitzgerald SW, Remer EM, Friedman H, Rogers LF, Hendrix RW, Schafer MF. MR evaluation of the anterior cruciate ligament: value of supplementing sagittal images with coronal and axial images. *AJR Am J Roentgenol* 1993;160:1233-1237
8. Peterfy CG, Gold G, Eckstein F, Cicuttini F, Dardzinski B, Stevens R. MRI protocols for whole-organ assessment of the knee in osteoarthritis. *Osteoarthritis Cartilage* 2006;14 Suppl A:A95-A111
9. Betts AM, Leach JL, Jones BV, Zhang B, Serai S. Brain imaging with synthetic MR in children: clinical quality assessment. *Neuroradiology* 2016;58:1017-1026
10. Blystad I, Warntjes JB, Smedby O, Landtblom AM, Lundberg P, Larsson EM. Synthetic MRI of the brain in a clinical setting. *Acta Radiol* 2012;53:1158-1163
11. Hasan KM, Walimuni IS, Abid H, Wolinsky JS, Narayana PA. Multi-modal quantitative MRI investigation of brain tissue neurodegeneration in multiple sclerosis. *J Magn Reson Imaging* 2012;35:1300-1311
12. West J, Warntjes JB, Lundberg P. Novel whole brain segmentation and volume estimation using quantitative MRI. *Eur Radiol* 2012;22:998-1007
13. Bonnier G, Roche A, Romascano D, Simioni S, Meskaldji D, Rotzinger D, et al. Advanced MRI unravels the nature of tissue alterations in early multiple sclerosis. *Ann Clin Transl Neurol* 2014;1:423-432
14. Granberg T, Uppman M, Hashim F, Cananau C, Nordin LE, Shams S, et al. Clinical feasibility of synthetic MRI in multiple sclerosis: a diagnostic and volumetric validation study. *AJNR Am J Neuroradiol* 2016;37:1023-1029
15. Masi JN, Sell CA, Phan C, Han E, Newitt D, Steinbach L, et al. Cartilage MR imaging at 3.0 versus that at 1.5 T: preliminary results in a porcine model. *Radiology* 2005;236:140-150
16. Barnett MJ. MR diagnosis of internal derangements of the knee: effect of field strength on efficacy. *AJR Am J Roentgenol* 1993;161:115-118
17. Mink JH, Levy T, Crues JV 3rd. Tears of the anterior cruciate ligament and menisci of the knee: MR imaging evaluation. *Radiology* 1988;167:769-774
18. Robertson PL, Schweitzer ME, Bartolozzi AR, Ugoni A. Anterior cruciate ligament tears: evaluation of multiple signs with MR imaging. *Radiology* 1994;193:829-834
19. De Smet AA, Norris MA, Yandow DR, Quintana FA, Graf BK, Keene JS. MR diagnosis of meniscal tears of the knee: importance of high signal in the meniscus that extends to the

- surface. *AJR Am J Roentgenol* 1993;161:101-107
20. Noyes FR, Stabler CL. A system for grading articular cartilage lesions at arthroscopy. *Am J Sports Med* 1989;17:505-513
 21. Landis JR, Koch GG. The measurement of observer agreement for categorical data. *Biometrics* 1977;33:159-174
 22. Barth M, Breuer F, Koopmans PJ, Norris DG, Poser BA. Simultaneous multislice (SMS) imaging techniques. *Magn Reson Med* 2016;75:63-81
 23. Zahneisen B, Ernst T, Poser BA. SENSE and simultaneous multislice imaging. *Magn Reson Med* 2015;74:1356-1362
 24. Zhang T, Chowdhury S, Lustig M, Barth RA, Alley MT, Grafendorfer T, et al. Clinical performance of contrast enhanced abdominal pediatric MRI with fast combined parallel imaging compressed sensing reconstruction. *J Magn Reson Imaging* 2014;40:13-25
 25. Warntjes JB, Dahlqvist O, Lundberg P. Novel method for rapid, simultaneous T1, T2*, and proton density quantification. *Magn Reson Med* 2007;57:528-537
 26. Nozaki T, Kaneko Y, Yu HJ, Kaneshiro K, Schwarzkopf R, Yoshioka H. Comparison of T1rho imaging between spoiled gradient echo (SPGR) and balanced steady state free precession (b-FFE) sequence of knee cartilage at 3T MRI. *Eur J Radiol* 2015;84:1299-1305
 27. Kijowski R, Blankenbaker DG, Munoz Del Rio A, Baer GS, Graf BK. Evaluation of the articular cartilage of the knee joint: value of adding a T2 mapping sequence to a routine MR imaging protocol. *Radiology* 2013;267:503-513
 28. Yoon MA, Hong SJ, Im AL, Kang CH, Kim BH, Kim IS. Comparison of T1rho and T2 mapping of knee articular cartilage in an asymptomatic population. *Korean J Radiol* 2016;17:912-918
 29. Oei EH, Nikken JJ, Verstijnen AC, Ginai AZ, Myriam Hunink MG. MR imaging of the menisci and cruciate ligaments: a systematic review. *Radiology* 2003;226:837-848
 30. Jung JY, Yoon YC, Kwon JW, Ahn JH, Choe BK. Diagnosis of internal derangement of the knee at 3.0-T MR imaging: 3D isotropic intermediate-weighted versus 2D sequences. *Radiology* 2009;253:780-787
 31. Jung JY, Yoon YC, Kim HR, Choe BK, Wang JH, Jung JY. Knee derangements: comparison of isotropic 3D fast spin-echo, isotropic 3D balanced fast field-echo, and conventional 2D fast spin-echo MR imaging. *Radiology* 2013;268:802-813
 32. Kijowski R, Davis KW, Woods MA, Lindstrom MJ, De Smet AA, Gold GE, et al. Knee joint: comprehensive assessment with 3D isotropic resolution fast spin-echo MR imaging--diagnostic performance compared with that of conventional MR imaging at 3.0 T. *Radiology* 2009;252:486-495
 33. Nguyen JC, De Smet AA, Graf BK, Rosas HG. MR imaging-based diagnosis and classification of meniscal tears. *Radiographics* 2014;34:981-999
 34. Pipe JG. Motion correction with PROPELLER MRI: application to head motion and free-breathing cardiac imaging. *Magn Reson Med* 1999;42:963-969